Indistinguishability of entangled photons generated with achromatic phase matching

Juan P. Torres,[1,2] Morgan W. Mitchell,[1] and Martin Hendrych[1,*]
[1]*ICFO-Institut de Ciencies Fotoniques, Universitat Politecnica de Catalunya, 08034 Barcelona, Spain*
[2]*Department of Signal Theory and Communications, Universitat Politecnica de Catalunya, 08034 Barcelona, Spain*
(Received 11 August 2004; published 28 February 2005)

We put forward a method to suppress distinguishing information contained in the frequency spectrum of entangled photon pairs generated in spontaneous parametric down-conversion. The distinguishing information is shown to be suppressed by employing achromatic phase-matching techniques to tailor the group velocities of the generated signal and idler photons, and thus tuning their spectral properties. The method can be implemented in materials and frequency bands where conventional solutions do not hold, and it can benefit from the dispersion cancellation inherent to entangled photons featuring frequency correlation or anticorrelation. The generation of polarization Bell states is discussed.

DOI: 10.1103/PhysRevA.71.022320 PACS number(s): 03.67.Mn, 42.50.Ar, 42.50.Dv, 42.65.Ky

Spontaneous parametric down-conversion (SPDC) provides pairs of photons entangled in frequency, in transverse momentum, in polarization or spin angular momentum, and in orbital angular momentum. Most quantum information applications, such as quantum teleportation and quantum cryptography, use polarization entanglement as the quantum resource [1–3]. The generation of the corresponding entangled states, which make use of only a portion of the total two-photon quantum state, requires the suppression of any distinguishing "which-path" information that otherwise degrades the degree of entanglement. For example, the actual generation of the Bell state $|\Psi^+\rangle = 1/\sqrt{2}(|H\rangle_1|V\rangle_2 + |V\rangle_1|H\rangle_2)$, where H and V refer, respectively, to horizontal and vertical polarization, requires the erasure of any space-time distinguishing information between the two components of the entangled state. The presence of distinguishing information can be revealed in a Hong-Ou-Mandel (HOM) interferometer [4,5], where a null of the fourth-order quantum interference is a signature of indistinguishability.

By and large, indistinguishable photon paths are not harvested directly at the output of the downconverting crystal; thus, elucidation of techniques to erase the distinguishing information is required. An illustrative example is the case of type-II (*eoe*) down-conversion with a continuous-wave pump beam, where the generated photons correspond to the ordinary and the extraordinary polarizations of the nonlinear crystal. Therefore, the emitted photons have different polarizations and thus different group velocities, making them distinguishable by their arrival times. However, under continuous-wave pumping the signal and idler generated photons turn out to be frequency anticorrelated, a property that makes it possible to erase the distinguishing information by imposing an appropriate time delay on one of the polarizations. Nevertheless, many applications require ultrashort pump pulses, and under such conditions the frequency anticorrelation is lost, rendering ineffective simple compensation strategies [6,7] and degrading the polarization entanglement. In this particular case, temporal distinguishing information can still be erased by making use of an entanglement concentration technique in the HOM interferometer [8], by using schemes involving multiple crystals [9] or multiple passes through the same crystal [10].

In general, the erasure of temporal distinguishing information can be achieved when the entangled photons are generated in highly frequency correlated or anticorrelated states [11], a situation that, however, can only occur in special crystals with suitable pump light conditions. For example, frequency-correlated photons, which do produce complete fourth-order interference in a HOM, can be obtained in a special nonlinear crystal where the group velocity of the pump beam happens to match the average group velocity of the down-converted photons [12,13]. Such conditions might not always exist or might not be convenient for a given application. Therefore, elucidation of techniques to expand the available possibilities is of paramount practical importance.

Here we show that achromatic phase-matching [14] techniques provide a powerful solution to tailor the degree of indistinguishability between the photons generated by SPDC, which can be applied in a wide variety of wavelengths and nonlinear materials. Achromatic phase matching has been used in second-harmonic generation configurations to increase the phase-matching bandwidth. This is achieved by introducing a spectral angular dispersion so that different spectral components propagate at their phase-matching angles. On physical grounds, the potential of this technique is based on the ability of achromatic phase-matching techniques to engineer the frequency correlations between the generated photons. Achromatic phase matching, or tilted-pulse techniques, pass the pump beam through a device with angular dispersion, such as a prism [15] or a diffraction grating [14,16], and henceforth employs the Poynting vector walk-off exhibited by nonlinear crystals outside noncritical phase matching to modify the effective group velocity and group velocity dispersion experienced by all involved photons.

Consider a second-order nonlinear optical crystal of length L, illuminated by a laser pump beam propagating in the z direction. The two-photon quantum state $|\Psi\rangle$ at the output of the nonlinear crystal, within first-order perturbation

*On leave from the Joint Laboratory of Optics, Palacky University, Olomouc, Czech Republic.

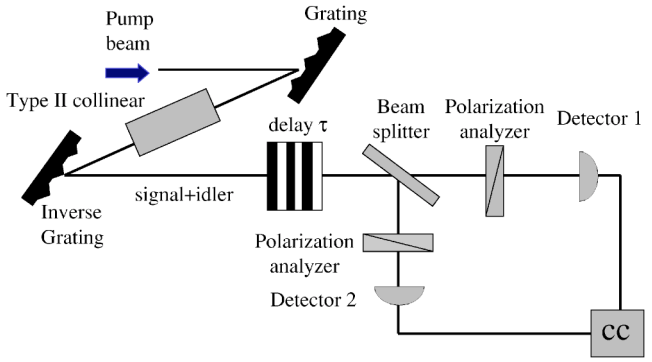

FIG. 1. Hong-Ou-Mandel experimental setup for observing two-photon fourth-order interference between a pair of photons in type-II down-conversion, under conditions for achromatic phase matching.

theory, is given by $|\Psi\rangle=|0,0\rangle-(i/\hbar)\int_0^\tau dt H_I(t)|0,0\rangle$, where $|0,0\rangle$ is the vacuum state, τ is the interaction time, and $H_I(t)$ is the effective Hamiltonian in the interaction picture, given by $H_I=\epsilon_0\int_V dV\,\chi^{(2)}\hat{E}_p^+\hat{E}_s^-\hat{E}_i^-+\text{H.c.}$, where ϵ_0 is the permittivity of free space, $\chi^{(2)}$ is the second-order nonlinear susceptibility tensor, V is the volume of the crystal illuminated by the pump beam, $\hat{E}_p^+$ refers to the positive-frequency part of the pump electric-field operator, which is treated classically, and $\hat{E}_{s,i}^-$ refer to the negative-frequency part of the signal and idler electric-field operators, respectively.

To achieve achromatic phase matching, let the input pump beam with frequency and transverse momentum distribution given by $E_0(\omega_0+\Omega,p_x,p_y)$ be diffracted by a grating located in front of the nonlinear crystal (see Fig. 1). Here $\mathbf{p}=(p_x,p_y)$ is the transverse momentum, ω_0 is the central angular frequency of the pump beam, and Ω is the angular frequency deviation from the central frequency. For simplicity, we assume normal incidence at the crystal. At the grating, each spectral component is dispersed in a different direction. For a grating oriented in the x direction, the output signal of the grating is a tilted pulse

$$E_0(\omega_0+\Omega,p_x,p_y)\rightarrow E_0(\omega_0+\Omega,p_x/\alpha-\Omega\tan(\varphi)/(\alpha c),p_y), \tag{1}$$

where φ is the tilt angle, $\alpha=-\cos\theta_0/\cos\beta_0$, θ_0 is the angle of incidence at the grating, β_0 is the output diffraction angle, and c is the velocity of light. The resulting pump beam is a tilted pulse, so that its peak intensity is located at a different time for each value of x. For normal incidence on the nonlinear crystal, one has [14] $\tan\varphi=-\lambda\epsilon$, where the angular dispersion ϵ of the grating is given by

$$\epsilon=\frac{m}{d\cos\beta_0}, \tag{2}$$

with d being the groove spacing of the grating and m the diffraction order. The pump beam that propagates inside the nonlinear crystal is given by

$$E_p^+(\mathbf{x},z,t)=\int d\omega_p d\mathbf{p}E_0(\omega_p,p_x/\alpha-\Omega_p\tan(\varphi)/(\alpha c),p_y)\times\exp\{ik_p z+i\mathbf{p}\cdot[\mathbf{x}+z\rho_p]-i\omega_p t\}, \tag{3}$$

where $\omega_p=\omega_0+\Omega_p$, $\mathbf{x}=(x,y)$ is the position in the transverse plane, $k_p(\omega_p,\mathbf{p})=[(\omega_p n_p/c)^2-|\mathbf{p}|^2]^{1/2}$ is the longitudinal wave number inside the crystal, n_p is the refractive index at the pump wavelength, and $\rho_p=(\rho_{0x},\rho_{0y})$ is the Poynting vector walk-off parameter of the pump beam due to the different propagation directions of energy and phase fronts inside the anisotropic nonlinear crystal.

We illustrate the potential of the technique described in this paper by focusing on the case of collinear type-II (*eoe*) downconversion in a uniaxial crystal where the optic axis is contained in the XZ plane, so that $\rho_p=(\rho_0,0)$. Such is the case of, e.g., β-barium borate (BBO) or lithium niobate ($LiNbO_3$). Under such conditions, the electric-field amplitude operator for the signal photon is given by

$$\hat{E}_s^-(\mathbf{x},z,t)\propto\int d\omega_s d\mathbf{p}\times\exp\{-ik_s z-i\mathbf{p}\cdot[\mathbf{x}+z\rho_s]+i\omega_s t\}\hat{a}_s^\dagger(\omega_s,\mathbf{p}), \tag{4}$$

where $\omega_s=\omega_0/2+\Omega_s$, $\mathbf{p}=(p_x,p_y)$ is the transverse momentum of the signal photon, $k_s(\omega_s,\mathbf{p})=[(\omega_s n_{s,i}/c)^2-|\mathbf{p}|^2]^{1/2}$ is the longitudinal wave number, $\hat{a}_s^\dagger$ is the creation operator for the signal photon with momentum $\mathbf{p}$ and frequency ω_s, n_s is the refractive index inside the nonlinear crystal at the signal wavelength, and $\rho_s=(\rho_1,0)$ is the walk-off parameter for the signal wave. The electric-field amplitude operator for the idler photon is similar, with $\mathbf{q}=(q_x,q_y)$ being the transverse momentum of the idler photon, $\rho_i=\mathbf{0}$, and $\omega_i=\omega_0/2+\Omega_i$.

At the output face of the nonlinear crystal ($z=L$), a second grating is used to recollimate the beam by compensating for the angular dispersion introduced by the first grating. Since the tilt imprinted on the pump beam is transferred to the mode function of the downconverted photons, this can be achieved by using a grating with parameters [17] $\alpha'=1/\alpha$ and $\epsilon'=-\epsilon/\alpha$. We assume that the gratings act only as dispersive elements, and not as frequency or angular filters. That is, we assume frequency- and angle-independent diffraction efficiencies. The effect of the second grating on the two-photon state function can be described by making the substitution $p_x\rightarrow\alpha p_x+\Omega_s\tan\varphi/c$, and $q_x\rightarrow\alpha q_x+\Omega_i\tan\varphi/c$. The quantum state of the photon pair at the output face of the nonlinear crystal can be written as

$$|\Psi\rangle=\int d\omega_s d\omega_i d\mathbf{p}d\mathbf{q}\Phi(\omega_s,\omega_i,\mathbf{p},\mathbf{q})\hat{a}_s^\dagger(\omega_s,\mathbf{p})\hat{a}_i^\dagger(\omega_i,\mathbf{q})|0,0\rangle, \tag{5}$$

where the state function is

$$\Phi(\omega_s,\omega_i,\mathbf{p},\mathbf{q})=E_0(\omega_s+\omega_i,\mathbf{p}+\mathbf{q})W(\Delta_k L/2). \tag{6}$$

The function $W(\Delta_k L/2)=\text{sinc}(\Delta_k L/2)\exp(i\Delta_k L/2)$ comes from the phase-matching condition along the longitudinal direction z. One finds

$$\Delta_k = k_p(\omega_s + \omega_i, \overline{p_x} + \overline{q_x}, p_y + q_y) + (\overline{p_x} + \overline{q_x})\tan\rho_0 - k_s(\omega_s, \overline{p_x}, p_y) - \overline{p_x}\tan\rho_1 - k_i(\omega_i, \overline{q_x}, q_y), \quad (7)$$

where $\overline{p_x} = \alpha p_x + \Omega_s \tan\varphi/c$ and $\overline{q_x} = \alpha q_x + \Omega_i \tan\varphi/c$. In each specific detection scheme—e.g., projection into Gaussian modes with single-mode optical fibers—Eq. (6) has to be integrated over the required spatial modes. Here we address the properties of the entangled states projected into spatial modes with large beam widths, by monitoring the function $\Psi(\Omega_s, \Omega_i) = \Phi(\Omega_s, \Omega_i, \mathbf{p}=\mathbf{0}, \mathbf{q}=\mathbf{0})$, a quantity that can be acquired experimentally with the signal and idler photons passing through an appropriate $2-f$ optical system. This is equivalent to spatial filtering of the mode function, which although it will reduce the number of photon pairs detected, allows us to consider only the frequency entanglement of the down-converted photons. Notwithstanding, no narrow-band filtering is required.

In the HOM detection scheme, the downconverted photons are incident on a nonpolarizing beam splitter with polarization analyzers at each output port. This device acts as a polarization HOM interferometer: If the signal and idler photons are indistinguishable, the two "paths" to coincidence detection interfere. The coincidence rate for detection of one photon at each one of the output ports of the HOM interferometer is given by

$$R(\tau) = \int d\Omega_1 \Omega_2 |\sin\theta_a \cos\theta_b f(\omega_1, \omega_2) + \cos\theta_a \sin\theta_b f(\omega_2, \omega_1) \exp\{-i(\Omega_1 - \Omega_2)\tau + i[k_s(\omega_2) - k_s(\omega_1) + k_i(\omega_1) - k_i(\omega_2)]L\}|^2, \quad (8)$$

where $k_{s,i}(\omega) \equiv k_{s,i}(\omega, \mathbf{p}=\mathbf{0})$, θ_a and θ_b are the polarization rotation angles of the analyzers located in each output port of the HOM interferometer, and $f(\omega_s, \omega_i) = \Psi(\omega_s, \omega_i)\mathcal{F}(\omega_s)\mathcal{F}(\omega_i)$ is the joint spectral amplitude multiplied by Gaussian spectral filters functions $\mathcal{F}$ associated with the filters located in front of the detectors.

In order to obtain complete destructive fourth-order interference in the HOM interferometer, the down-converted photons should be highly frequency correlated or frequency anticorrelated. The nature of the frequency correlations between the down-converted photons is given by the loci of perfect phase matching in the (Ω_s, Ω_i) plane of the joint spectral spectral intensity $|\Psi(\Omega_s, \Omega_i)|^2$ [7]. In our scheme, this quantity turns out to be determined by the tilt angle of the angularly dispersed pump beam. To make this readily apparent, let [6] $k_s \approx k_s^0 + N_s\Omega_s, k_i \approx k_i^0 + N_i\Omega_i$, and $k_p \approx k_p^0 + N_p\Omega_p$. Under this approximation, perfect phase matching is achieved for signal and idler frequencies that verify

$$\frac{\Omega_i}{\Omega_s} = -\frac{N_p + \tan\varphi\tan\rho_0/c - N_s - \tan\varphi\tan\rho_1/c}{N_p + \tan\varphi\tan\rho_0/c - N_i}. \quad (9)$$

Frequency-correlated photons are obtained for tilt angles such that $\Omega_s = \Omega_i$, while frequency-anticorrelated photons correspond to the case $\Omega_s = -\Omega_i$.

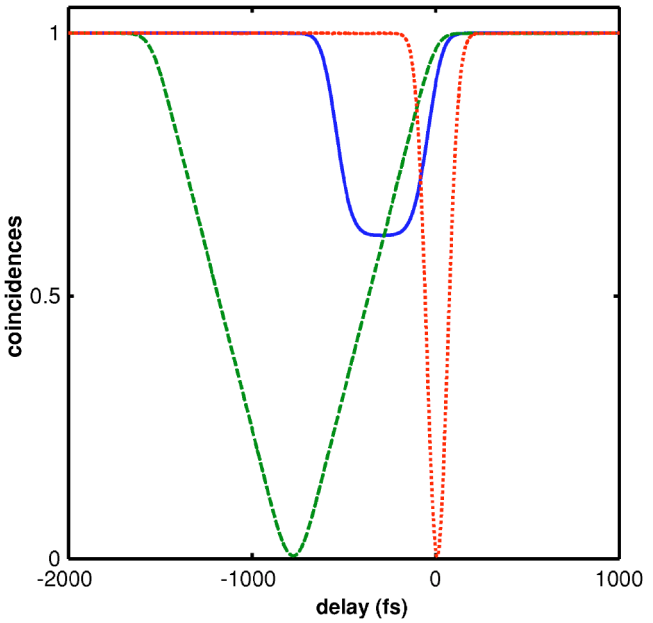

FIG. 2. Normalized coincidence rate as a function of temporal delay τ, for three different values of the tilt angle of the pump pulse. Solid line: $\varphi = 0°$. Dashed line: $\varphi = -53.1°$, which corresponds to highly correlated photons. Dotted line: $\varphi = 39.6°$, which corresponds to highly anticorrelated photons. Phase-matching angle $\theta = 42.3°$, temporal pulse width $T_0 = 100$ fs, crystal length $L = 3$ mm, and filter bandwidth $\Delta\lambda = 10$ nm.

In Fig. 2, we plot the behavior obtained for the coincidences $R(\tau)$ as a function of the time delay, for the cases of highly frequency-correlated and frequency-anticorrelated photons generated with achromatic phase matching. The case of a pump beam with no tilt is also shown for the sake of comparison. In this particular plot, the polarization angle of the analyzers is set to $\theta_a = -\theta_b = \pi/4$. Calculations were performed for a pump pulse with a Gaussian shape—i.e., $E_0 \propto \exp[-\Omega_p^2 T_0^2/(8\ln 2)]$, where $T_0 = 100$ fs is the pulse temporal width [full width at half maximum (FWHM) at intensity]. We consider a degenerate type-II SPDC process in a BBO nonlinear crystal pumped at a frequency-doubled Ti:sapphire, laser ($\lambda_p^0 \sim 400$ nm) [18]. The Gaussian spectral filters were set to $\mathcal{F} \propto \exp[-(2\ln 2)\Omega_{s,i}^2/\sigma^2]$, where σ is the FWHM width. In such case, frequency-anticorrelated photons are obtained with a tilt angle $\varphi \simeq 39.6°$, while frequency-correlated photons are obtained with a tilt angle $\varphi \simeq -53.1°$.

In the case of frequency-correlated photons, the delay τ_0 that gives a null of the coincidences rates can be obtained from Eq. (9) by considering $\Omega_s = \Omega_i$, so that

$$\tau_0 \approx (N_s + \tan\rho_1\tan\varphi/c - N_i)\frac{L}{2}, \quad (10)$$

as is also obtained numerically from minimizing $R(\tau)$ in Eq. (8). This result can be understood by noticing that the signal photon, due to the angular dispersion of the pump beam, propagates with an effective inverse group velocity given by $N_s' = N_s + \tan\rho_1\tan\varphi/c$ [19]. One also finds that, because of the negligible spatial walk-off for this polarization, the idler

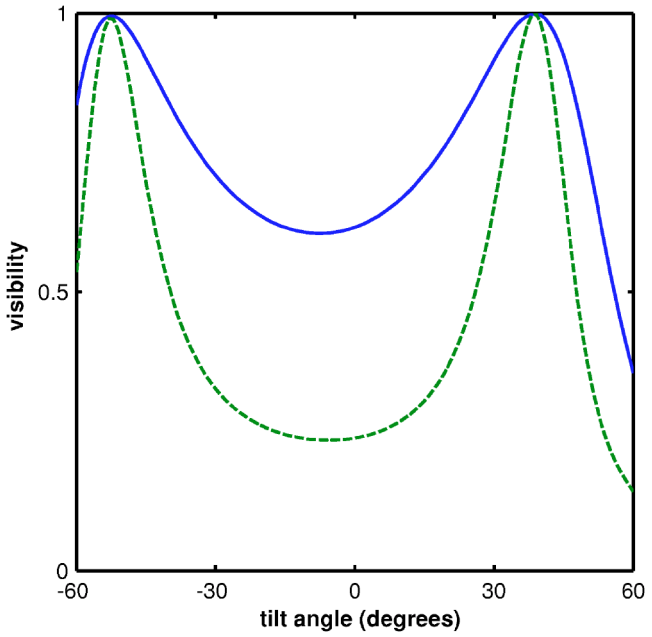

FIG. 3. Visibility of the coincidence rate curve as a function of the tilt angle. Solid line: $L=1.5$ mm. Dashed line: $L=3$ mm. Phase-matching angle $\theta=42.3°$, temporal pulse width $T_0=100$ fs, and filter bandwidth $\Delta\lambda=10$ nm. The tilt angle is given in degrees.

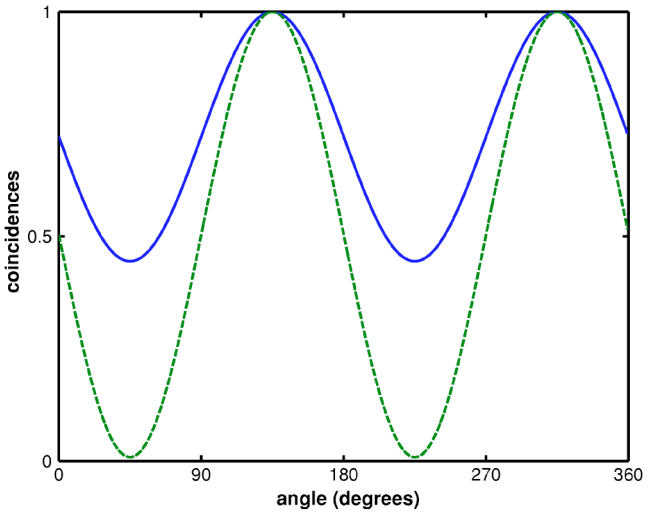

FIG. 4. Coincidence rate as a function of the polarization angle θ_b for fixed $\theta_a=-\pi/4$. Solid line: no tilt and delay $\tau_0=-294$ fs. Dashed line: tilt angle $\phi=-53.1°$, which correspond to highly correlated photons, with delay $\tau_0=-774$ fs. With a tilt angle $\phi=39.6°$, which corresponds to highly anticorrelated photons, with delay $\tau_0=0$, one also obtains the dashed curve. Phase-matching angle $\theta=42.3°$, temporal pulse width $T_0=100$ fs, filter bandwidth $\Delta\lambda=10$ nm, and crystal length $L=3$ mm.

photon does not modify its inverse group velocity, so that $N_i'=N_i$. Therefore, with Eq. (10) one recovers formally the delay required for obtaining destructive fourth-order interference, and therefore temporal indistinguishability between both photons, in a HOM interferometer for type-II down-conversion driven by a cw pump beam [20]. Under the particular material and pump conditions mentioned above, one obtains $\tau\approx-784$ fs, while without tilt one has $\tau\approx-300$ fs. For the case of frequency-anticorrelated photons, the delay is zero.

Next we discuss the visibility of the fourth-order interference as a function of the tilt angle. The central results are illustrated in Fig. 3. Maximum visibility is obtained at tilts that correspond to the generation of highly frequency-correlated and frequency-anticorrelated photons. Notice also that similar results, not shown here, are obtained with other crystal parameters and pump light wavelengths than those displayed.

Importantly, the scheme proposed here can be used to generate polarization entanglement with a broadband pump. Type-II down-conversion produces photon pairs in a product state of one horizontal and one vertical photon. In the cases where the photons are split into different output ports, they emerge in the Bell state $|\Psi^+\rangle$, but only if they do not contain any spectral or temporal distinguishing information. In Fig. 4 we plot the coincidence rate as a function of the angle of one of the polarizers (θ_b). The successful erasure of all distinguishing temporal information for the generation of a polarization entangled state requires that the coincidence rate behave as $R(\theta_a,\theta_b,\tau_0)\propto\sin^2(\theta_a+\theta_b)$, where τ_0 is the value of the delay that produces complete destructive interference in the HOM interferometer. The plot in Fig. 4 shows the coincidence rate for the case with $\theta_a=-\pi/4$, showing that effectively the scheme proposed here can act as a polarization entanglement generator. Similar results are obtained with other values of the polarization angles of the analyzers.

In conclusion, we stress the potential of achromatic phase-matching techniques to suppress all temporal distinguishing information between photons generated in SPDC. The method provides a powerful tool to expand the frequency bands and nonlinear materials where specific frequency correlations between the pair of photons are required. Moreover, the method described here can also benefit from the dispersion cancellation effect that appears for entangled two-photons states when the two photons are frequency correlated or anticorrelated [12,21]. Diffraction gratings with suitable groove spacing to produce the required tilted pulses are readily available.

This work was supported by the Generalitat de Catalunya and by Grant No. BFM2002-2861 from the Government of Spain.

[1] *The Physics of Quantum Information*, edited by D. Bouwmeester, A. Ekert, and A. Zeilinger (Springer, Berlin, 2000).
[2] D. Bouwmeester, J. W. Pan, K. Mattle, M. Eibl, H. Weinfurter, and A. Zeilinger, Nature (London) **390**, 575 (1997).
[3] N. Gisin, G. Ribordy, W. Tittel, and H. Zbinden, Rev. Mod. Phys. **74**, 145 (2002).
[4] C. K. Hong, Z. Y. Ou, and L. Mandel, Phys. Rev. Lett. **59**, 2044 (1987).
[5] Y. H. Kim and W. P. Grice, Phys. Rev. A **68** 062305 (2003).
[6] T. E. Keller and M. H. Rubin, Phys. Rev. A **56**, 1534 (1997).
[7] W. P. Grice and I. A. Walmsley, Phys. Rev. A **56**, 1627 (1997).
[8] Y. H. Kim, S. P. Kulik, M. V. Chekhova, W. P. Grice, and Y. Shih, Phys. Rev. A **67**, 010301 (2003).
[9] Y. H. Kim, S. P. Kulik, and Y. Shih, Phys. Rev. A **62**, 011802 (2000).
[10] D. Branning, W. P. Grice, R. Erdmann, and I. A. Walmsley, Phys. Rev. Lett. **83**, 955 (1999).
[11] A. B. U'Ren, K. Banaszek, and I. A. Walmsley, Quantum Inf. Comput. **3**, 480 (2003).
[12] R. Erdmann, D. Branning, W. Grice, and I. A. Walmsley, Phys. Rev. A **62**, 053810 (2000).
[13] V. Giovannetti, L. Maccone, J. H. Shapiro, and F. N. Wong, Phys. Rev. Lett. **88**, 183602 (2002).
[14] O. E. Martinez, IEEE J. Quantum Electron. **25**, 2464 (1989).
[15] V. D. Volosov, S. G. Karpenko, N. E. Kornienko, and V. L. Strizhevskii, Sov. J. Quantum Electron. **4**, 1090 (1975).
[16] G. Szab and Z. Bor, Appl. Phys. B: Photophys. Laser Chem. **50**, 51 (1990).
[17] O. E. Martinez, J. Opt. Soc. Am. B **3**, 929 (1986).
[18] V. G. Dmitriev, G. G. Gurzadyan, and D. N. Nikogosyan, *Handbook of Nonlinear Optical Crystals* (Springer, Berlin, 1997).
[19] J. P. Torres, S. Carrasco, L. Torner, and E. W. VanStryland, Opt. Lett. **25**, 1735 (2000).
[20] M. H. Rubin, D. N. Klyshko, Y. H. Shih, and A. V. Sergienko, Phys. Rev. A **50**, 5122 (1994).
[21] A. M. Steinberg, P. G. Kwiat, and R. Y. Chiao, Phys. Rev. Lett. **68**, 2421 (1992).